

# Nonlinear Equation for Flexural Stiffness of Slender Composite Columns in Major Axis Bending

Timo K. Tikka, M.ASCE<sup>1</sup>; and S. Ali Mirza, F.ASCE<sup>2</sup>

**Abstract:** The ACI standard 318-02 permits the use of a moment magnifier approach for the design of slender composite steel-concrete columns. This approach is strongly influenced by the effective flexural stiffness ( $EI$ ), which varies due to the nonlinearity of the concrete stress-strain curve and the cracking along the column length among other factors. The  $EI$  equations given in the ACI code are approximate when compared to the  $EI$  values computed from the axial load-bending moment-curvature relationships. This study was undertaken to determine the influence of a full range of variables on  $EI$  used for the design of slender, tied, composite columns in which steel shapes are encased in concrete, and also to examine the existing ACI  $EI$  equations. Approximately 12,000 isolated square composite columns, each with a different combination of specified properties of variables, were simulated and used to generate the stiffness data. The columns studied were subjected to short-term ultimate loads and equal and opposite end moments causing symmetrical single curvature bending about the major axis of the encased steel section. A new nonlinear equation for  $EI$  was then developed for use in design of slender composite columns subjected to major axis bending and is proposed as an alternative to the existing ACI  $EI$  equations.

**DOI:** 10.1061/(ASCE)0733-9445(2006)132:3(387)

**CE Database subject headings:** Building codes; Composite structures; Loads; Stiffness; Structural design; Concrete columns; Steel columns.

## Introduction

The American Concrete Institute building code ACI 318-02 (2002) permits the use of a moment magnifier approach for computing the second-order moments in slender composite columns. This approach was introduced into design practice to eliminate the need for extensive calculations, based on the solution to a differential equation, to compute second-order bending moments in columns, and is influenced by the critical buckling load ( $P_c$ ). The computation of  $P_c$  is strongly influenced by the effective flexural stiffness ( $EI$ ), which varies due to the nonlinearity of the concrete stress-strain curve, creep, and cracking along the height of the column. The  $EI$  expressions given in ACI 318-02 [2002, Eq. (10-21) and Eq. (10-12)] for composite columns are quite approximate when compared to values derived from the axial load, bending moment, and curvature ( $P-M-\phi$ ) relationships. In addition, the ACI  $EI$  equations currently in use were developed for reinforced concrete columns subjected to high axial loads and were simply modified, without any further investigation, for use in composite column design (Mirza and Tikka 1999a).

This study was undertaken to determine the influence of a full range of variables on the short-term effective flexural stiffness ( $EI$ ) of slender, tied, composite columns in which the bending moment was applied about the major axis of the steel section encased in concrete; to examine the existing expressions for  $EI$ ; to develop and propose a refined expression for  $EI$ ; and to compare the proposed expression for  $EI$  with the current ACI expressions for such columns. Approximately 12,000 isolated composite columns were simulated to generate the stiffness data to study the effects of a number of variables that affect the effective flexural stiffness. Each simulated column had a different combination of cross section, geometric, and material properties. The columns bent about the major axis of the encased steel section in symmetrical single curvature in braced frames subjected to short-term loads. The moment magnifier approach specified in the ACI code was developed for these types of columns. The effects of different loading conditions, end restraints, and lateral supports are accounted for in the ACI code through the use of the equivalent uniform bending moment diagram factor ( $C_m$ ), effective length factor ( $K$ ), and sustained load factor ( $\beta_d$ ). The columns studied are graphically represented in Fig. 1 and were chosen because the errors in  $C_m$ ,  $K$ , and  $\beta_d$  would not affect the accuracy of the  $EI$  expression developed later in this paper.

A nonlinear  $EI$  equation is proposed for computing the flexural stiffness of composite columns subjected to bending about the major axis of the encased steel section. Statistical evaluations of parameters affecting the flexural stiffness show that the variability of the proposed equation is less than one-third of that associated with the current ACI  $EI$  expressions for the design of slender composite steel-concrete columns. A graphical design aid developed for computing  $EI$  from the proposed equation is also included in this paper.

<sup>1</sup>Assistant Professor, Civil Engineering, Lakehead Univ., Thunder Bay, Ontario, Canada P7B 5E1.

<sup>2</sup>Professor Emeritus, Civil Engineering, Lakehead Univ., Thunder Bay, Ontario, Canada P7B 5E1.

Note. Associate Editor: Jin-Guang Teng. Discussion open until August 1, 2006. Separate discussions must be submitted for individual papers. To extend the closing date by one month, a written request must be filed with the ASCE Managing Editor. The manuscript for this paper was submitted for review and possible publication on January 19, 2005; approved on March 25, 2005. This paper is part of the *Journal of Structural Engineering*, Vol. 132, No. 3, March 1, 2006. ©ASCE, ISSN 0733-9445/2006/3-387-399/\$25.00.

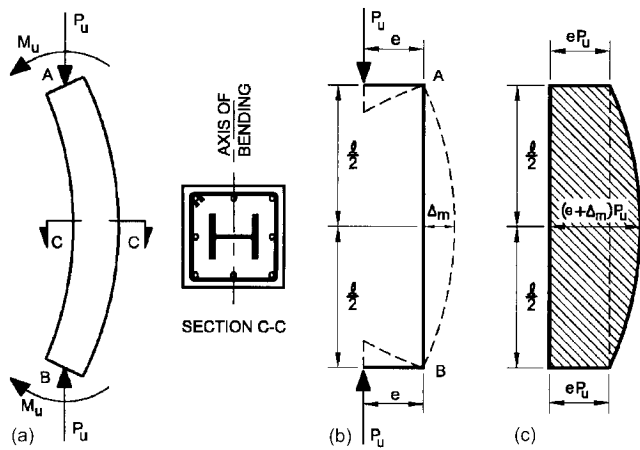


Fig. 1. Type of composite column studied: (a) free-body diagram of pin-ended column in symmetrical single-curvature bending; (b) forces on column; and (c) bending moment diagram ( $M_u = eP_u$ )

### Method Used for Evaluating Theoretical Flexural Stiffness

ACI 318-02 permits the use of a moment magnifier approach to compute the maximum bending moment ( $M_{max}$ ), which includes second-order effects, occurring along the height of a column

$$M_{max} = M_c = \delta_{ns} M_2 = C_m \delta_1 M_2 \geq M_2 \quad (1)$$

where  $\delta_{ns}$  = moment magnifier for columns that are part of braced (nonsway) frames;  $M_2$  = larger of the two factored end moments ( $M_1$  and  $M_2$ ) computed from a conventional elastic frame analysis and is always taken as positive;  $C_m$  = equivalent uniform moment diagram factor; and  $\delta_1$  = moment magnifier for the same columns when subjected to axial load and equal and opposite (equivalent) end moments causing symmetrical single curvature bending. For this study  $M_1$  and  $M_2$  are equal and opposite causing symmetric single curvature bending; therefore,  $C_m = 1.0$ .

Chen and Lui (1987) explain that the moment magnifier  $\delta_1$  for pin-ended columns subjected to end moments can be derived from the basic differential equation governing the elastic in-plane behavior of a column and is reproduced in the following equation

$$\delta_1 = \sqrt{\frac{2(1 - \cos k\ell)}{\sin^2 k\ell}} \quad (2)$$

where  $\ell$  = column length; and  $k$  = lowest eigenvalue solution to the basic differential equation of equilibrium

$$k = \frac{\pi}{\ell} \sqrt{\frac{P_u}{P_{cr}}} \quad (3)$$

where  $P_u$  = factored axial load acting on the column; and  $P_{cr}$  = Euler's buckling strength for a pin-ended column which is given by

$$P_{cr} = \frac{\pi^2 EI}{\ell^2} \quad (4)$$

For design purposes, the ACI 318-02 has adopted the simplified and widely accepted approximation of Eq. (2)

$$\delta_1 = \frac{1}{1 - \frac{P_u}{P_c}} \quad (5)$$

where  $P_c$  = critical load and is computed as

$$P_c = \frac{\pi^2 EI}{(K\ell)^2} \quad (6)$$

For this study, however, the effective length factor  $K=1.0$  and  $P_c$  is reduced to Euler's buckling strength equation [Eq. (4)] for a pin-ended column.

The moment magnifier method defined by Eqs. (1), (5), and (6) is described graphically in Fig. 2, which shows the relationship between the cross section axial load-bending moment strength interaction diagram and the column strength interaction diagram for pin-ended columns in symmetrical single curvature bending. Fig. 2 shows that, for a given axial load  $P_u$ , the column end moment  $M_2$  at point A is multiplied by  $\delta_1$  to obtain  $M_{max}$  at point B. The current  $EI$  expressions used by ACI 318-02 were developed for use with Eqs. (1), (5), and (6).

### Development of Theoretical Stiffness Equation Used for this Study

The bending moment relationship (secant formula) for a pin-ended slender column subjected to equal and opposite end moments is given by Timoshenko and Gere (1961) as

$$M_c = M_2 \sec\left(\frac{\pi}{2} \sqrt{\frac{P_u}{P_{cr}}}\right) \quad (7)$$

where  $M_c$  = design bending moment that includes second-order effects;  $M_2$  = applied column end moment calculated from a conventional elastic analysis;  $P_u$  = factored axial load acting on the column; and  $P_{cr}$  = Euler's buckling strength [Eq. (4)]. For the purpose of analysis,  $M_c$  and  $M_2$  are replaced by the cross section bending moment strength  $M_{cs}$  and the overall column bending moment strength  $M_{col}$ , respectively. Substituting Euler's buckling strength [Eq. (4)] into Eq. (7), then rearranging, simplifying, and solving for  $EI$  gives the following expression for the theoretical

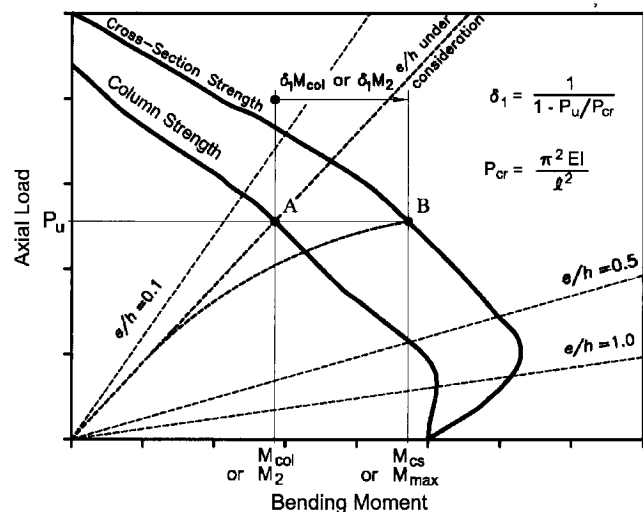


Fig. 2. Schematic composite cross section and column (member) ultimate axial load-bending moment interaction diagrams

flexural stiffness of a pin-ended column subjected to symmetrical single curvature bending

$$EI_{th} = \frac{P_u \ell^2}{4 \left[ \arccos \left( \frac{M_{cs}}{M_{col}} \right) \right]^2} \quad (8)$$

The computations of the terms  $P_u$ ,  $M_{cs}$ , and  $M_{col}$  used in this expression were based on the cross section and column axial load-bending moment ( $P$ - $M$ ) interaction diagrams explained in the following section. A full derivation for  $EI_{th}$  is documented by Mirza (1990).

### Computations of Theoretical Cross Section and Slender Column Bending Moment Resistances

The strength of a composite cross section was represented by an axial load-bending moment interaction diagram, similar to the one shown in Fig. 2. A strain-compatibility and force-equilibrium solution was used to generate the moment-curvature curves for different levels of axial load acting on the composite cross section. The maximum bending moment  $M_{cs}$  from the moment-curvature curve for a given axial load level  $P_u$  defined one point on the cross section strength interaction diagram. When the moment-curvature curves were completed for the desired axial load levels, the maximum bending moment for each axial load level was stored to define the entire interaction diagram for the cross section. Forty-eight points (axial load levels) were used to accurately define the entire cross section strength interaction diagram.

The strength of a slender pin-ended composite column subjected to end moments producing symmetrical single curvature bending was also represented by an axial load-bending moment interaction diagram, as shown in Fig. 2. The column bending moment capacity  $M_{col}$ , or the end moment  $M_2$ , for a given axial load was calculated using a numerical iterative procedure that computed second-order bending moments and deflections along the length of the column by incrementing the end moments until the maximum moment along the length of the column reached the maximum moment on the cross section moment-curvature curve for the given axial load. The column axial load strength  $P_u$  and the corresponding computed value of  $M_{col}$  represented one point on the column  $P$ - $M$  interaction curve (Fig. 2).

Newmark's method (1943) was used to determine the equilibrium configuration for a given combination of axial load and end moments that were applied to the column. The column was subdivided into segments or stations of equal length for which initial deflections were assumed based on the applied end moments. The first-order moments, and the second-order moments caused by slenderness effects, were computed and summed at each station. The curvature corresponding to the total moment at each station was retrieved from the cross section moment-curvature curve for the given axial load level in order to define the distribution of curvature along the column length. The conjugate beam method was then used to compute the deflection at each of the stations in an iterative manner. If the computed deflections and the initial deflections were within the prescribed limits of 0.05%, an equilibrium solution had been obtained. If not, the computed deflections were substituted for the assumed deflections and the process was repeated until the deflections converged. The end moments were then incremented equally and the process was repeated until the maximum bending moment ( $M_{max}$ ) calculated along the length of the member reached the maximum moment on the cross section moment-curvature curve for the axial load under consider-

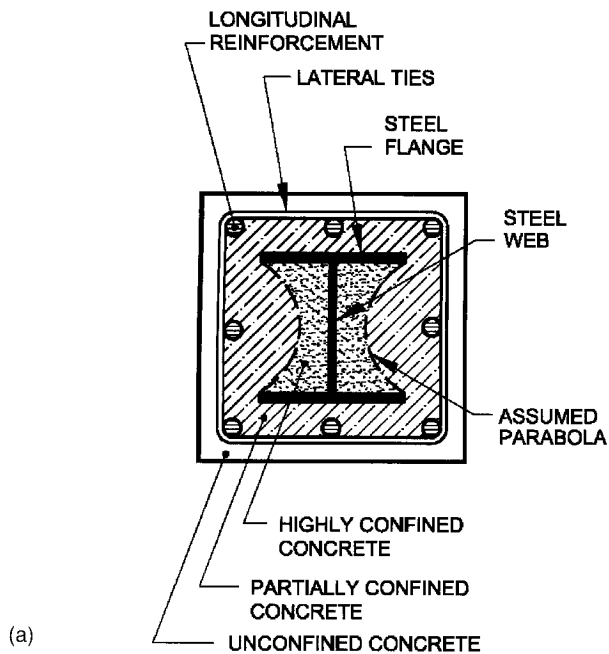
ation. The maximum end moment  $M_{col}$  ( $M_2$ ) corresponding to  $M_{cs}$  ( $M_{max}$ ) for each axial load level was stored to define the entire interaction diagram for the slender column. The number of points (axial load levels) used to define the slender column interaction diagram ranged from approximately 32 points, for  $\ell/h=30$ , to 45 points, for  $\ell/h=10$ . The computed values of  $M_{cs}$  and  $M_{col}$  for each column (with  $\ell$  and  $P_u$  for given  $e/h$  ratios) were then used directly in Eq. (8) to compute the theoretical  $EI$ .

The major assumptions used in determining the axial load-moment-curvature ( $P$ - $M$ - $\phi$ ) relationship,  $M_{cs}$  and  $M_{col}$ , were: (1) strains between concrete, structural steel, and reinforcing steel were compatible and no slip occurred; (2) the strain was linearly proportional to the distance from the neutral axis; (3) concrete and steel stresses were functions of strains; (4) the confinement of the concrete provided by lateral ties and the structural steel section was considered; (5) the effects of residual stresses in the steel section were included; and (6) the strain hardening of steel was neglected. Note that previous studies by Mirza and Skrabek (1991, 1992) show that the effects of strain hardening become significant for short columns ( $\ell/h=0$ ) when  $e/h > 1$  and for long columns ( $\ell/h > 20$ ) when  $e/h > 4$ .

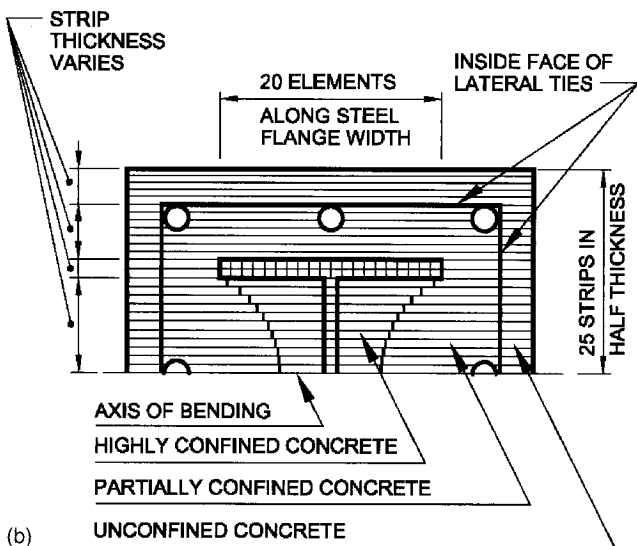
A composite column cross section was assumed to consist of three materials [Fig. 3(a)]: concrete, structural steel, and longitudinal reinforcing steel. The concrete was divided into three types: unconfined concrete outside the lateral ties, highly confined concrete between the steel section web and flanges, and partially confined concrete inside the lateral ties but outside the influence of the steel section. The boundary between the partially and highly confined concretes was described by a parabola, as suggested by Mirza and Skrabek (1991). The steel section was subdivided into two parts, the web and the flanges, to account for differences in residual stresses. Therefore, six different stress-strain curves were used to represent the materials in the cross section, which was divided into strips and elements as shown in Fig. 3(b).

A modified Kent-and-Park stress-strain relationship (Park et al. 1982) was used for concrete in compression. The ascending portion of the curve was described by a second-order parabola, and the descending branch of the curve beyond the maximum strength was described by a straight line. The slope of the descending branch for unconfined concrete depended on the concrete strength. For the partially confined concrete, the slope of the descending branch was affected by the concrete strength as well as the level of confinement provided by the lateral ties. For the highly confined concrete, the slope of the straight line was arbitrarily assumed to be zero due to the confinement provided by the partially confined concrete on one side and the steel section web and flanges on the remaining sides. The assumed zones of concrete confinement are shown in Fig. 3. Concrete in tension was represented by a linear, brittle stress-strain relationship with the maximum tensile strength represented by the modulus of rupture.

An elastic-plastic stress-strain relationship was assumed for both the structural and reinforcing steels. A linear distribution of the residual stresses was assumed for the web and flanges of the steel section. The expression suggested by Young (1971) to compute the residual stress at the flange tips was combined with the expression suggested by Galambos (1963) for computing the residual stress at flange-web junctures. Further details are documented in earlier studies (Mirza and Skrabek 1991, 1992) and will not be repeated here.



(a)



(b)

**Fig. 3.** (a) Details of composite cross section used and (b) discretization of one-half composite cross section used for computing theoretical strength

### Experimental Verification of Theoretical Strength Procedure

To test the accuracy of the strength procedure, the strengths computed by the theoretical model were compared to the strengths of 30 physical tests available in the literature. These tests were conducted on composite columns for which the bending moment in symmetrical single-curvature was applied about the major axis of the encased steel section and were taken from Johnson and May (1978), Morino et al. (1984), Procter (1967), Roik and Mangerig (1987), Roik and Schwalbenhofer (1988), and Suzuki et al. (1984). The ratio of test to computed strengths for the 30 composite columns ( $e/h=0.11$  to  $1.06$ ,  $\ell/h=3.8$  to  $28.9$ ,  $\rho_{rs}=0.0$  to  $0.8\%$ ,  $\rho_{ss}=4.2$  to  $14.5\%$ ) ranged from  $0.84$  to  $1.18$  with an average value of  $1.02$  and a coefficient of variation of  $9\%$ .

The frequency histogram of the strength ratios for these speci-

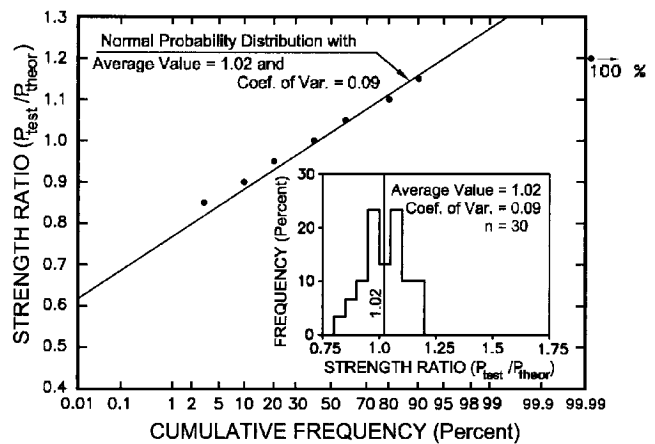


**Fig. 4.** Probability distribution of ratios of tested to theoretically computed strengths of 30 composite column specimens subjected to symmetrical single curvature bending about the major axis of the encased steel section

mens is plotted on the inset of Fig. 4. The cumulative frequency curve of the strength ratios for the same data is plotted also in Fig. 4 on a normal probability paper and is compared with a normal probability distribution using the same average value and coefficient of variation as those obtained from the test data. Based on the plots of Fig. 4 and statistics of strength ratios given on the inset of Fig. 4, it can be assumed that the strength ratio of composite columns subjected to symmetrical single curvature bending is normally distributed with an average value of  $1.02$  and coefficient of variation of  $0.09$ . This indicates a good correlation between the theoretical model and composite column test results. Furthermore, an earlier study (Tikka and Mirza 2004) also found this strength model to be reasonably accurate for physical tests conducted on 146 reinforced concrete columns subjected to combined axial load and symmetrical single curvature bending.

### Simulation of Theoretical Stiffness Data for Columns Studied

Approximately 12,000 isolated composite steel-concrete columns subjected to bending about the major axis of the encased steel section were simulated for this study. Each column had a different combination of specified properties. The specified concrete strengths  $f'_c$ , longitudinal reinforcing steel ratios  $\rho_{rs}$ , and structural steel ratios  $\rho_{ss}$  listed in Table 1 represent the usual ranges of these variables used in the construction industry. All columns had reinforcing steel with a specified yield strength  $f_{yrs}$  of  $414$  MPa ( $60$  ksi) and  $13$  mm ( $0.5$  in.) diameter lateral ties spaced at  $280$  mm ( $11$  in.) and conforming to ACI Building Code sections 10.16.8.3–10.16.8.5. The structural steel sections with three different specified yield strengths  $f_{yrs}$  were used. The clear concrete cover on lateral ties was held constant at  $38$  mm ( $1.5$  in.) for this study. Five slenderness ratios  $\ell/h$  were chosen to represent the range of  $\ell/h$  permitted by ACI 318-02, clause 10.11, for columns in braced frames. Table 1 shows that eleven end eccentricity ratios  $e/h$  ranging from  $0.05$  to  $1.0$  were used. Note that for concrete buildings  $e/h$  usually ranges from  $0.1$  to  $0.65$  (Mirza and MacGregor 1982). The overall dimensions of the composite cross section were held constant at  $560$  mm  $\times$   $560$  mm ( $22$  in.  $\times$   $22$  in.) because a previous parametric study concluded

**Table 1.** Specified Properties of Composite Columns Studied

Properties	Specified values	Number of specified values
$f'_c$ MPa (psi)	27.6; 34.5; 41.4; 55.2 (4000; 5000; 6000; 8000)	4
$f_{ys}$ MPa (psi)	248; 303; 345 (36,000; 44,000; 50,000)	3
$\rho_{fs}$ (percent)	1.09; 1.96; 3.17	3
Structural steel	Section $\rho_{ss}$ (percent)	6
	W310×253 10.33	
	W310×179 7.29	
	W310×107 4.36	
	W250×167 6.80	
	W250×101 4.13	
	W200×100 4.07	
$\ell/h$	10; 15; 20; 25; 30	5
$e/h$	0.05; 0.1; 0.2; 0.3; 0.4; 0.5; 0.6; 0.7; 0.8; 0.9; 1.0	11

Note: The number of simulated composite columns subjected to major axis bending equals  $(4 \times 3 \times 3 \times 6 \times 5 \times 11 =)$  11,880 with each column having a different combination of specified properties shown above. Overall dimensions of the concrete cross section were 560×560 mm (22×22 in.) with lateral ties 13 mm (0.5 in.) in diameter spaced at 280 mm (11 in.) center-to-center, clear cover to lateral ties 38 mm (1.5 in.), and specified yield strength of reinforcing steel bars  $f_{ys}$  414 MPa (60 ksi). Imperial equivalents of the steel sections noted above are W12×170, W12×120, W12×72, W10×112, W10×68, and W8×67, respectively.

that the overall cross section size was not a major variable for investigating the reliability of strength and stiffness of composite columns (Mirza 1989).

The theoretical  $EI$  for each of the columns studied was computed from Eq. (8) using  $M_{cs}$  from the cross section strength interaction diagram and  $M_{col}$  from the slender column interaction diagram.

### Examination of ACI Stiffness Equations

ACI 318-02 [2002, Eq. (10–21) and Eq. (10–12)] permits the use of Eqs. (9) and (10) for calculating the effective flexural stiffness ( $EI$ ) of slender composite columns

$$EI = \frac{0.2E_cJ_g}{(1 + \beta_d)} + E_sI_{ss} \quad (9)$$

$$EI = \frac{0.4E_cJ_g}{(1 + \beta_d)} \quad (10)$$

where  $E_c$  and  $E_s$ =moduli of elasticity of concrete and steel;  $J_g$  and  $I_{ss}$ =moments of inertia of the gross concrete cross-section and the structural steel section taken about the centroidal axis of the composite column cross-section; and  $\beta_d$ =the sustained load factor taken as the ratio of the maximum factored axial dead load to the total factored axial load (for the type of column studied) and is always positive. For short-term loads,  $\beta_d=0$ , and Eqs. (9) and (10) are simplified to Eqs. (11) and (12), respectively

$$EI = 0.2E_cJ_g + E_sI_{ss} \quad (11)$$

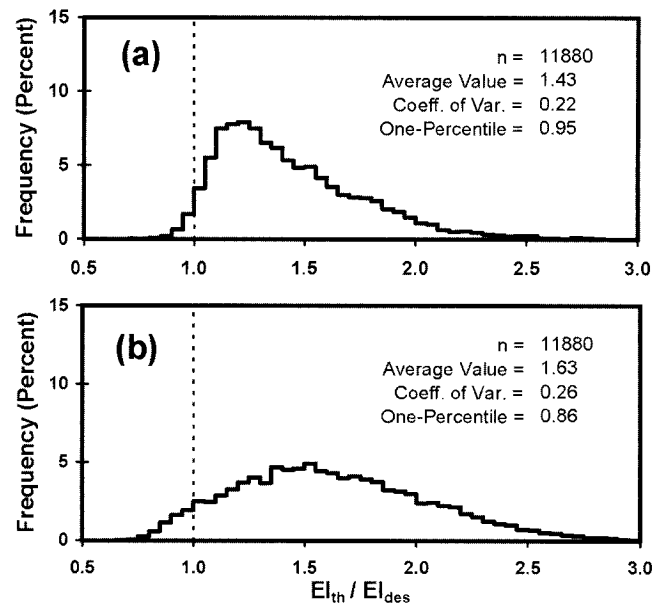


**Fig. 5.** Comparison of ACI stiffness equations with theoretical results: (a) Eq. (11) [ACI 318-02, Eq. (10–21)] and (b) Eq. (12) [ACI 318-02, Eq. (10–12)].

$$EI = 0.4E_cJ_g \quad (12)$$

Note that in Eqs. (9)–(12),  $E_s$  was taken as 200,000 MPa (29,000,000 psi) and  $E_c$  was computed from  $4,700\sqrt{f'_c}$  MPa ( $57,000\sqrt{f'_c}$  psi), as specified in ACI 318-02.

Eqs. (11) and (12) were compared with the theoretical  $EI$  values computed from Eq. (8) for all simulated composite columns. The results of these comparisons are plotted in Figs. 5(a and b), respectively, which show histograms and statistics of the ratios of theoretical  $EI$  to ACI design  $EI$  ( $EI_{th}/EI_{des}$ ). Stiffness ratios ( $EI_{th}/EI_{des}$ ) greater than one signify that  $EI_{des}$  is conservative, and values of  $EI_{th}/EI_{des}$  less than one indicate that  $EI_{des}$  is nonconservative.

Fig. 5 shows that, on the average, the stiffness values obtained from both ACI equations are less than the theoretical values and are generally conservative. However, the relatively high coefficients of variation obtained for both of these equations [22% for Eq. (11) and 26% for Eq. (12)] indicate that, for a significant number of columns studied, the ACI  $EI$  deviated substantially from the corresponding theoretically computed  $EI$ . These inaccuracies are the consequences of both ACI equations [Eqs. (11) and (12)] using a constant value of the coefficient (0.2 or 0.4) assigned to  $E_cJ_g$  as well as ignoring the contribution of longitudinal steel bars to the effective flexural stiffness, and of Eq. (12) also ignoring the contribution of structural steel section to the effective flexural stiffness, regardless of different parameters that affect the strength of slender composite steel-concrete columns. It is evident from histograms shown in Fig. 5 that there appears to be a need for modification in the existing ACI  $EI$  equations for the type of columns studied. Similar conclusions were reached by Mirza and Tikka (1999a,b).

### Development of Proposed Equation for Short-Term Effective Flexural Stiffness

The  $EI$  of a slender composite steel-concrete column is significantly affected by cracking along its length and by inelastic be-

havior of the concrete and structural and reinforcing steels.  $EI$  is, therefore, a complex function of a number of variables that cannot be readily transformed into a unique and simple analytical expression, such as Eqs. (11) and (12). In this study, the proposed stiffness equation was developed through the following steps: (1) a format of the proposed  $EI$  equation was selected that included variables affecting  $EI$  significantly; (2) a multiple linear regression analysis of the generated theoretical  $EI$  data was conducted to evaluate coefficients related to some of the variables included in the proposed  $EI$  equation; and (3) the proposed  $EI$  equation was then finalized by curve fitting to one-percentile values of the generated theoretical stiffness data. This procedure was used since the objective was to develop a more accurate but relatively simple  $EI$  equation.

### Format of and Variables Used for Proposed Effective Flexural Stiffness Equation

As pointed out previously, the inaccuracies in Eq. (11) are introduced because the contribution of the longitudinal reinforcing bars is ignored and because a constant value of the coefficient equal to 0.2 is assigned to  $E_c I_g$  regardless of different parameters that affect the stiffness. The variables used for the development of the  $EI$  equation proposed in this study were divided into two groups: (1) variables affecting the contribution of concrete ( $E_c I_g$ ) to the overall effective stiffness; and (2) variables affecting the contribution of structural steel ( $E_s I_{ss}$ ) and of longitudinal reinforcing steel ( $E_s I_{rs}$ ) to the overall effective stiffness. Therefore, a modified version of Eq. (11) is proposed that takes the form

$$EI = \alpha_c E_c (I_g - I_{ss}) + \alpha_{ss} E_s I_{ss} + \alpha_{rs} E_s I_{rs} \quad (13)$$

where  $\alpha_c$ ,  $\alpha_{ss}$ , and  $\alpha_{rs}$  = dimensionless reduction factors (effective stiffness factors) for concrete, structural steel, and longitudinal reinforcing steel, respectively; and  $I_{rs}$  = moment of inertia of the longitudinal reinforcing steel bars taken about the centroidal axis of the composite cross-section. The reduction factor  $\alpha_c$  represents the effects of several variables that influence the contribution of concrete to the overall column stiffness and can be a linear or nonlinear function of these variables. Therefore, Eq. (13) can be developed as a linear or nonlinear equation. If  $\alpha_c$  is taken as a linear function of  $x_1$  and  $x_2$  and assumed to be equal to  $(\alpha_k + \alpha_1 x_1 + \alpha_2 x_2)$ , Eq. (13) becomes

$$EI = (\alpha_k + \alpha_1 x_1 + \alpha_2 x_2) E_c (I_g - I_{ss}) + \alpha_{ss} E_s I_{ss} + \alpha_{rs} E_s I_{rs} \quad (14)$$

where  $\alpha_k$  is a constant (equivalent to the intercept of a simple linear equation) and the remaining  $\alpha$  values are dimensionless factors corresponding to independent variables  $x_1$ ,  $x_2$ ,  $E_s I_{ss}$ , and  $E_s I_{rs}$ .

Earlier studies (Mirza and Tikka 1999a,b) investigated a large number of variables and concluded that only a few variables had significant effects on the contribution of the concrete part of the cross section to the stiffness of slender composite columns. A correlation analysis of the theoretical  $EI$  data simulated for this study indicated that  $e/h$  or  $e/h$  combined with  $\ell/h$  have the most significant effect on the contribution of concrete to the stiffness of slender composite columns. Similar findings were reported by Mirza (1990) and Mirza and Tikka (1999a,b). Hence, Eq. (14) will assume the following form

$$EI = \left( \alpha_k + \alpha_1 \frac{e}{h} + \alpha_2 \frac{\ell}{h} \right) E_c (I_g - I_{ss}) + \alpha_{ss} E_s I_{ss} + \alpha_{rs} E_s I_{rs} \quad (15)$$

To simplify the analysis of the theoretical stiffness data, Eq. (15) was nondimensionalized by dividing both sides by  $E_c (I_g - I_{ss})$ . The nondimensionalized linear equation for  $EI$  is

$$\frac{EI}{E_c (I_g - I_{ss})} = \alpha_k + \alpha_1 \frac{e}{h} + \alpha_2 \frac{\ell}{h} + \alpha_{ss} \frac{E_s I_{ss}}{E_c (I_g - I_{ss})} + \alpha_{rs} \frac{E_s I_{rs}}{E_c (I_g - I_{ss})} \quad (16)$$

Note that  $E_c$  and  $E_s$  values in Eq. (16) were taken the same as would be used by a designer and are given after Eq. (12).

### Regression Analysis of Theoretical Stiffness Data

A multiple linear regression analysis of the simulated theoretical stiffness data was conducted using Eq. (16). The  $EI$  values in Eq. (16) were taken from the simulated theoretical flexural stiffnesses computed from Eq. (8), and coefficients  $\alpha_k$ ,  $\alpha_1$ ,  $\alpha_2$ ,  $\alpha_{ss}$ , and  $\alpha_{rs}$  were computed from the regression analysis. The accuracy of an  $EI$  regression equation was based on the multiple correlation coefficient  $R_c$ , an index of the relative strength of the relationship, and the standard error  $S_e$  (a measure of sampling variability). An  $R_c$  value equal to zero signifies no correlation, and  $R_c = \pm 1.0$  indicates 100% correlation;  $R_c$  values greater than +1.0 and less than -1.0 are not possible. The smaller the value of  $S_e$ , the smaller is the sampling variability of the regression equation. Note that  $S_e$  in this study was computed for  $\alpha_k$ . The corresponding regression equations are

$$EI = \left( 0.332 - 0.202 \frac{e}{h} + 0.0028 \frac{\ell}{h} \right) E_c (I_g - I_{ss}) + 0.818 E_s I_{ss} + 0.802 E_s I_{rs} \quad (n = 11880; R_c = 0.965; S_e = 0.051) \quad (17)$$

$$EI = \left( 0.388 - 0.202 \frac{e}{h} \right) E_c (I_g - I_{ss}) + 0.818 E_s I_{ss} + 0.802 E_s I_{rs} \quad (n = 11880; R_c = 0.959; S_e = 0.054) \quad (18)$$

Both Eqs. (17) and (18) show that as the  $e/h$  ratio increases, there is a corresponding decrease in  $EI$  for a column. This is expected, because an increase in  $e/h$  means a corresponding increase in bending moment and in the outer fiber tension stresses, resulting in more cracking of the column. Eq. (17) also indicates that as the  $\ell/h$  ratio increases, there is an increase in  $EI$ . Mirza (1990) suggests that this is perhaps because the cracks are likely to be more widely spaced in a longer column with more concrete in between the cracks contributing to the stiffness of the column. Note that the theoretical procedure used in this study assumes that the concrete between the cracks does not provide additional stiffness in the cracked element(s) of a column. The coefficients  $\alpha_{ss}$  and  $\alpha_{rs}$  related to  $E_s I_{ss}$  and  $E_s I_{rs}$  in Eqs. (17) and (18) are less than unity and represent "softening" in stiffness due to the elastic-plastic nature of the stresses developed in the structural steel and longitudinal reinforcing steel bars near ultimate load.

### Proposed Design Equation

The regression analyses of the theoretical stiffness data described in the foregoing section were used to estimate values of coefficients related to some of the variables that affect the flexural stiffness of composite columns. Eqs. (17) and (18) show a constant value of  $\alpha_{ss} = 0.818$  and  $\alpha_{rs} = 0.802$ . Hence, a value of 0.8 for both  $\alpha_{ss}$  and  $\alpha_{rs}$  appears to be a reasonable approximation and was used for developing a more "refined"  $EI$  equation through

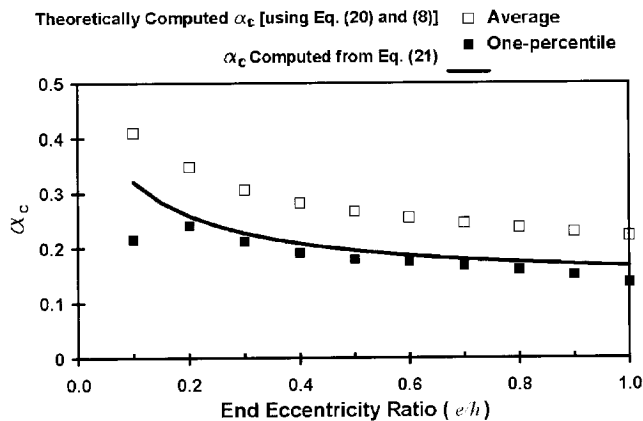


**Fig. 6.** Comparison of Eq. (21) with theoretically computed average and one-percentile values of  $\alpha_c$  for composite columns subjected to  $e/h$  ranging from 0.1 to 1.0 ( $n=1080$  for each  $e/h$  value plotted)

curve fitting to the simulated theoretical stiffness data. Substituting 0.8 for  $\alpha_{ss}$  and  $\alpha_{rs}$  in Eq. (13) yields the following expression

$$EI = \alpha_c E_c (I_g - I_{ss}) + 0.8 E_s (I_{ss} + I_{rs}) \quad (19)$$

where  $\alpha_c$  is a function of  $e/h$ , or  $e/h$  combined with  $\ell/h$ , depending on whether one ( $e/h$ ) or both ( $e/h$  and  $\ell/h$ ) of these variables are included in the analysis. Solving Eq. (19) for  $\alpha_c$  gives the following equation

$$\alpha_c = \frac{EI - 0.8 E_s (I_{ss} + I_{rs})}{E_c (I_g - I_{ss})} \quad (20)$$

Again,  $E_c$  and  $E_s$  values in Eq. (20) were taken the same as given after Eq. (12).

The theoretical values of  $\alpha_c$  were computed for all simulated columns for which  $e/h$  ranged from 0.1 to 1.0 by substituting the theoretical  $EI$  values obtained from Eq. (8) into Eq. (20). The averages (open square symbols) and one-percentiles (solid square symbols) of  $\alpha_c$  values so computed are plotted against the end eccentricity ratio in Fig. 6. The plots in Fig. 6 indicate that a nonlinear equation for  $\alpha_c$  is needed to fit the data.

A widely accepted and reasonable practice is to use either the five-percentile or one-percentile values for the development of design equations. A nonlinear equation for  $\alpha_c$  was visually fitted, with the aid of a spreadsheet, as close as possible to the one-percentile values of  $\alpha_c$  shown in Fig. 6. Using only  $e/h$  initially as a variable, the following equation for  $\alpha_c$  was obtained

$$\alpha_c = 0.5 - 3.5 \frac{e}{h} \left( \frac{1}{1 + 9.5 \frac{e}{h}} \right) \quad (21)$$

In Fig. 6, Eq. (21) is superimposed on the plots of theoretical values of  $\alpha_c$ . As expected, Eq. (21) shows an excellent agreement with most of the one-percentile values of theoretical  $\alpha_c$ , but is a conservative representation of the average values of theoretical  $\alpha_c$ .

In Eq. (17), the value of the coefficient  $\alpha_2$  associated with  $\ell/h$  is 0.0028. The coefficient  $\alpha_2$  was rounded to 0.003 and then used to modify Eq. (21) for including the effect of  $\ell/h$ . Based on a statistical analysis of the theoretical  $\alpha_c$  values for all simulated columns in which  $e/h$  ranged from 0.1 to 1.0, the following equation was selected for  $\alpha_c$ :

$$\alpha_c = 0.47 - 3.5 \frac{e}{h} \left( \frac{1}{1 + 9.5 \frac{e}{h}} \right) + 0.003 \frac{\ell}{h} \quad (22)$$

It is interesting to note that Eq. (22) reduces to Eq. (21) at  $\ell/h=10$ .

Substituting  $\alpha_c$  from Eq. (22) into Eq. (19) gives the following expression for  $EI$

$$EI = \left[ 0.47 - 3.5 \frac{e}{h} \left( \frac{1}{1 + 9.5 \frac{e}{h}} \right) + 0.003 \frac{\ell}{h} \right] E_c (I_g - I_{ss}) + 0.8 E_s (I_{ss} + I_{rs}) \quad (23)$$

Eq. (23) is the proposed design expression for short-term  $EI$  of slender composite steel-concrete columns under major axis bending and is subject to the following limitations:  $e/h \geq 0.1$ ;  $\ell/h \leq 30$ ;  $\rho_{rs} \geq 1\%$ ; and  $\rho_{ss} \geq 4\%$ . When  $e/h$  is less than 0.1, use  $e/h=0.1$  in Eq. (23). Note that this limitation on  $e/h$  was not included in statistical analyses of stiffnesses or stiffness ratios obtained from Eq. (23), and is presented later in Figs. 7–10 and 12.

A comparison of stiffnesses from the proposed design equation [Eq. (23)] with theoretical stiffnesses [Eq. (8)] for all simulated columns is shown in Fig. 7. Note that  $EI_{des}$  and  $EI_{th}$  plotted in Fig. 7 have been nondimensionalized by dividing them by  $E_c (I_g - I_{ss})$ . As expected, Eq. (23) produced reasonable correlation with the theoretical  $EI$  values.

## Analysis and Discussion of Simulated Results

Frequency histograms and other statistical data presented in this section were prepared for the stiffness ratios ( $EI_{th}/EI_{des}$ ) using different design equations. For computing the stiffness ratio,  $EI_{th}$  was taken as the simulated theoretical stiffness while  $EI_{des}$  was

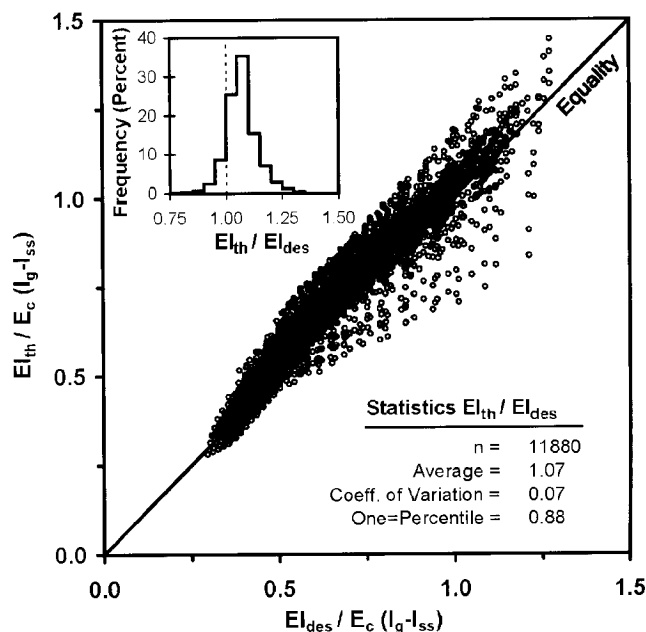


**Fig. 7.** Comparison of Eq. (23) with simulated theoretical  $EI$  data

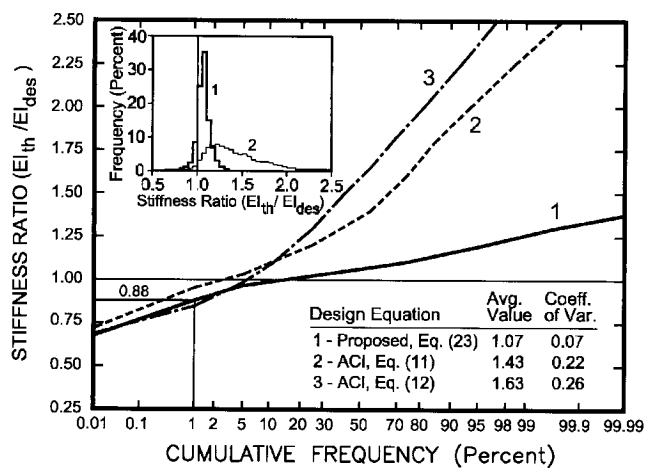


Fig. 8. Probability distributions of stiffness ratios computed from data for all composite columns ( $n=11,880$ )

computed from one of the ACI design equations [Eq. (11) or (12)] or from the proposed design equation [Eq. (23)].

### Overview of Stiffness Ratio Statistics

The frequency histogram and statistics shown in Fig. 7 were prepared using the proposed design equation [Eq. (23)]. A comparison of the histogram in Fig. 7 with those in Fig. 5(a and b) plotted for the ACI design equations can be summarized as follows:

1. The coefficient of variation of stiffness ratios for the proposed design equation is significantly lower—over 68% lower—than the values obtained from the ACI design equations.
2. The average stiffness ratios for the ACI design equations tend to be more conservative than that for the proposed design equation. However, the one-percentile stiffness ratios obtained for ACI design equations and for the proposed design equation are approximately the same.

These trends are more clearly seen by comparing cumulative frequency curves of stiffness ratios for the proposed and ACI design equations plotted on a normal probability paper in Fig. 8. The curves in Fig. 8 were prepared from the data for all of the columns studied. These curves indicate that the proposed design equation produces the least variable results for the columns studied, whereas ACI design equations produce stiffness ratios that are, in a large number of cases, significantly higher than 1.0. The same conclusions can be reached by comparing the histograms of stiffness ratios plotted on the inset of Fig. 8.

### Effects of Major Variables on Stiffness Ratios

The effects of the end eccentricity ratio ( $e/h$ ), axial load ratio ( $P_u/P_o$ ), slenderness ratio ( $\ell/h$ ), and longitudinal reinforcement ratio ( $\rho_{rs}$ ) on the average and one-percentile values of stiffness ratios ( $EI_{th}/EI_{des}$ ) obtained from ACI and proposed design equations [Eqs. (11), (12), and (23)], are shown in Figs. 9(a–d), respectively. Note that  $P_o$  in this study was defined as the unfactored pure axial load strength of a cross section and was computed from  $P_o=0.85f'_c(A_g-A_{ss}-A_{rs})+f_{y,ss}A_{ss}+f_{y,rs}A_{rs}$ , where  $A_g$ ,  $A_{ss}$ ,  $A_{rs}$ =areas of the gross concrete cross section, of the structural steel section, and of the longitudinal reinforcing steel bars.

Each of these figures were plotted from the data for all 11,880 columns studied. Following are conclusions that can be drawn from these figures.

1. The average and one-percentile stiffness ratios for the proposed design equation [Eq. (23)] are not significantly affected by  $e/h$ ,  $P_u/P_o$ ,  $\ell/h$ , and  $\rho_{rs}$ , whereas such values for the ACI equations [Eqs. (11) and (12)] are significantly affected by most of the same variables. This is expected for the ACI equations, because the ACI equations, particularly Eq. (12), do not include most of the variables studied.
2. The average stiffness ratios for the ACI design equations are very high in some cases. The ACI simple equation [Eq. (12)] produces the lowest one-percentile stiffness ratios over almost the entire range of  $\ell/h$  studied as well as for  $e/h>0.4$ . These trends for the ACI design equations are expected because the ACI expressions were developed originally for reinforced concrete columns subjected to low-end eccentricities and were applied to composite column design with some modification [Eq. (11)] or no modification [Eq. (12)].
3. The proposed design equation computes the effective flexural stiffnesses close to the theoretical values. The average and one-percentile values for the proposed design equation are above 1.0 and 0.85, respectively, for almost all of the cases studied.

The histograms and related statistics of stiffness ratios at each value of  $e/h$  studied are examined in Fig. 10 for the proposed equation. Fig. 10 clearly demonstrates that the end eccentricity ratio has virtually no effect on the histograms and related statistics of stiffness ratios for individual  $e/h$  values ranging from 0.1 to 1.0. This indicates that the proposed design equation adequately addresses the effect of  $e/h$ . Note that similar plots prepared using the ACI equations [Eqs. (11) and (12)], but not presented here, demonstrated substantial effects of the end eccentricity ratio.

### Stiffness Ratios Produced by Proposed Design Equation for Usual Columns

The end eccentricity ratio  $e/h$  for columns in concrete buildings usually ranges from 0.1 to 0.65 (Mirza and MacGregor 1982). In a survey of 22,000 columns conducted in the late 1960s by MacGregor et al. (1970), 99% had a slenderness ratio  $\ell/h \leq 20$ . Therefore, those columns for which  $e/h=0.1, 0.2, 0.3, 0.4, 0.5, 0.6$ , or  $0.7$  and  $\ell/h=10, 15$ , or  $20$  were defined as usual columns for this part of the study.

The average and minimum values of the stiffness ratios ( $EI_{th}/EI_{des}$ ) computed using Eq. (23) are plotted against  $e/h$  in Fig. 11(a) for  $\ell/h=10$  and in Fig. 11(b) for  $\ell/h=20$ . The one-percentile values are not plotted in these figures because the sample size for each point plotted ranges from 36 to 108 with minimum values representing 2.8 to 0.9 percentiles, respectively. Figs. 11(a and b) show that for almost all columns plotted, the minimum values exceed 0.85, and the average values are above 1.0.

Based on Fig. 11, the following conclusions appear to be valid for usual composite steel-concrete columns subjected to major axis bending ( $e/h=0.1$  to  $0.7$ ,  $\ell/h=10$  to  $20$ , and  $\rho_{ss}=4.2$  to  $10.3\%$ ):

1. The proposed design equation [Eq. (23)] does not introduce significant variations in stiffness ratios due to changes in  $e/h$ ,  $\ell/h$ , and  $\rho_{ss}$ ; and
2. The average and minimum stiffness ratios produced by Eq. (23) may be taken as at least 1.0 and 0.85, respectively.

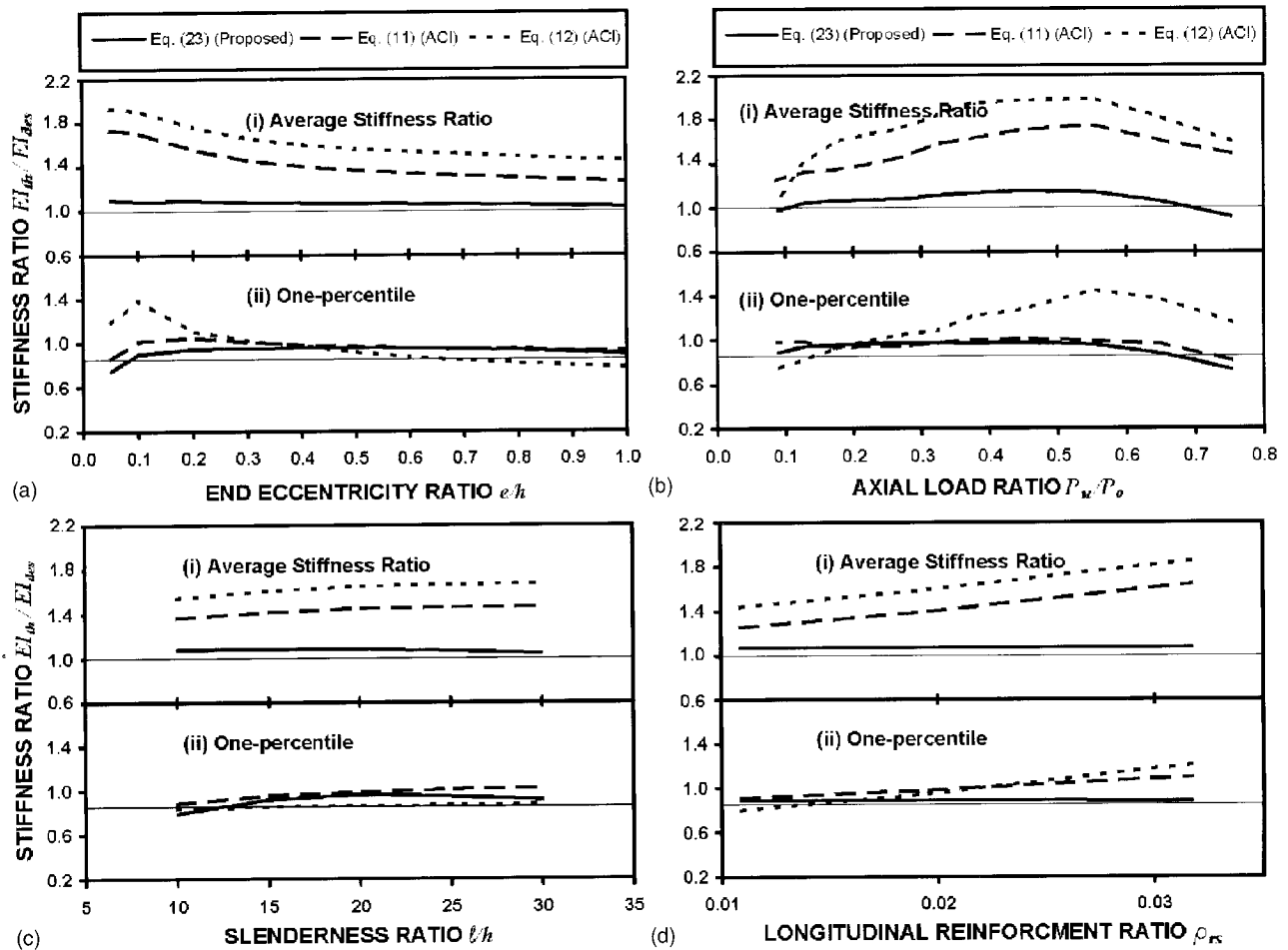


**Fig. 9.** Effects of variables on stiffness ratios for different design equations: (a) end eccentricity ratio ( $n=1,080$  for each of the eleven  $e/h$  ratios studied); (b) axial load ratio ( $n$  varies for each  $P_u/P_o$  ratio studied); (c) slenderness ratio ( $n=2,376$  for each of the five  $l/h$  ratios studied); and (d) longitudinal reinforcement ratio ( $n=3,960$  for each of the three  $\rho_{rs}$  ratios studied)

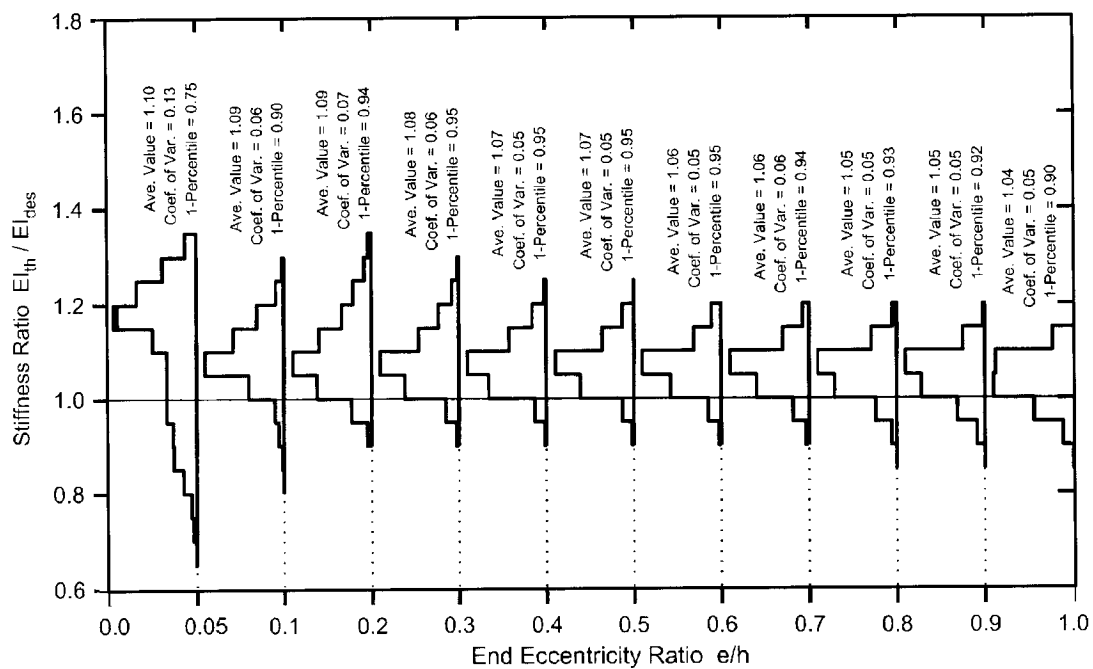


**Fig. 10.** Histograms of stiffness ratios plotted for composite columns at different end eccentricity ratios using the proposed design equation [Eq. (23)] ( $n=1,080$  for each  $e/h$  ratio studied)

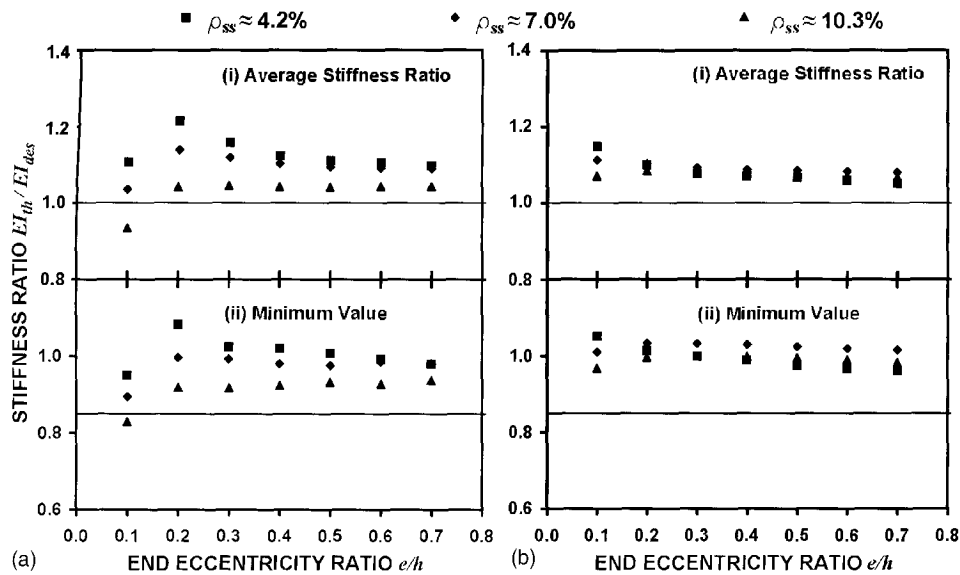


Fig. 11. Stiffness ratios obtained from the proposed design equation [Eq. (23)] for usual composite columns with: (a)  $l/h=10$ ; and (b)  $l/h=20$  (for each combination of  $e/h$  and  $\rho_{ss}$  ratios plotted,  $n=108$  when  $\rho_{ss} \approx 4.2\%$ ;  $n=72$  when  $\rho_{ss} \approx 7.0\%$ ; and  $n=36$  when  $\rho_{ss} \approx 10.3\%$ )

### Stiffness Reduction Factor for Proposed Equation

MacGregor (1976) suggested that the one-percentile strength ratios can be used to estimate the resistance reduction factors. The one-percentile stiffness ratios computed using the proposed  $EI$  equation [Eq. (23)] were 0.88 for all columns studied (Figs. 7 and 8). In addition, the plots investigating the effects of variables on stiffness ratios shown in Fig. 9 indicate that, in almost all cases,

the one-percentile values of stiffness ratios produced by Eq. (23) exceed 0.85. Hence, a stiffness reduction factor  $\phi_K=0.85$  is proposed for use when computing the factored critical buckling strength using the proposed  $EI$  equation [Eq. (23)] for composite columns subjected to bending about the major axis of the encased steel section. This value of  $\phi_K$  is higher than the 0.75 currently specified in ACI 318-02 (2002), which was originally computed

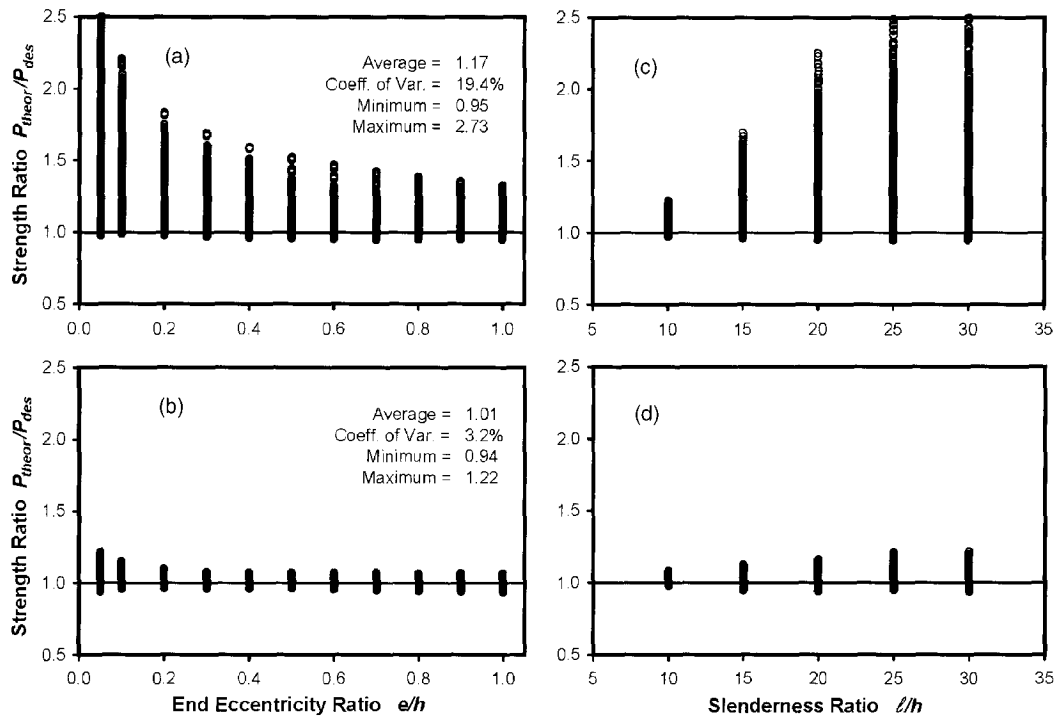


Fig. 12. Ratios of theoretically computed strengths to the strengths calculated from the moment magnifier approach using: (a) and (c), Eq. (11); and (b) and (d), Eq. (23) ( $n=1,080$  for each of the eleven  $e/h$  ratios studied, and  $n=2,376$  for each of the five  $l/h$  ratios studied)

by Mirza et al. (1987) for reinforced concrete columns subjected to short term loads using the ACI 318-02 Eq.(10-11) with  $\beta_d=0$ .

### Comparison of Column Strengths Based on ACI and Proposed Effective Flexural Stiffness Equations

Because  $EI$  is an intermediate step in the process of strength design of slender columns, the ultimate strengths of all 11,880 composite columns used in this study were computed from the moment magnifier approach using the ACI and proposed  $EI$  equations [Eq. (11) and Eq. (23)] and compared to the theoretically simulated strengths of the same columns. Hence, for the strength ratios ( $P_{theor}/P_{des}$ ) plotted against  $e/h$  and  $\ell/h$  in Fig. 12,  $P_{theor}$  was taken as the theoretically simulated strength, whereas  $P_{des}$  was computed from the moment magnifier approach using either Eq. (11) or Eq. (23). Note that the strength ratios and related statistics shown in Fig. 12 are based on unfactored strengths with  $\phi=\phi_K=1.0$  in all cases.

Figs. 12(a and c) show a large spread in strength ratios when the current ACI  $EI$  equation [Eq. (11)] is used in the moment magnifier approach. These strength ratios tend to become more scattered and more conservative at lower  $e/h$  and higher  $\ell/h$  ratios. On the other hand, Figs. 12(b and d) show that the scatter in the strength ratios almost disappears when the proposed  $EI$  equation [Eq. (23)] is used in the moment magnifier approach and the strength ratios appear to be independent of  $e/h$  or  $\ell/h$ . The strength ratio statistics computed using the ACI  $EI$  equation [Eq. (11)] and the proposed  $EI$  equation [Eq. (23)], shown in Figs. 12(a and b), respectively, also indicate that the proposed  $EI$  equation produces far more accurate results than does the current ACI  $EI$  equation. This is expected because  $e/h$  and  $\ell/h$  are both included as variables in Eq. (23).

### Design Application for Columns in Frames Subjected to Sustained Loads

The effects of sustained loads on the stiffness of composite columns can be accounted for by applying the sustained load factor  $\beta_d$  to Eq. (23) in a similar manner, as currently done in ACI 318-02 (2002)

$$EI = \frac{\alpha_c E_c (I_g - I_{ss})}{(1 + \beta_d)} + 0.8 E_s (I_{ss} + I_{rs}) \quad (24)$$

in which  $\alpha_c$  is computed from

$$\alpha_c = \left[ 0.47 - 3.5 \frac{e}{h} \left( \frac{1}{1 + 9.5 \frac{e}{h}} \right) + 0.003 \frac{\ell}{h} \right] \geq 0$$

Eq. (24) is the proposed design expression for slender composite columns subjected to sustained loads and is subject to the following limitations:  $e/h \geq 0.1$ ;  $\ell/h \leq 30$ ;  $\rho_{ss} \geq 4\%$ ; and  $\rho_{rs} \geq 1\%$ . When  $e/h$  is less than 0.1, use  $e/h=0.1$  in Eq. (24). In Eq. (24),  $e$  is the larger end eccentricity  $=M_2/P_u$ ;  $\ell$ =unsupported height of the column; and  $E_c$ ,  $E_s$ , and  $\beta_d$  values are the same as those given in ACI 318-02. For short-term loads ( $\beta_d=0$ ), Eq. (24) reduces to Eq. (23).

The effects of moment gradient and end restraints on columns in braced frames are accounted for in the ACI moment magnifier approach through the use of the equivalent uniform moment diagram factor  $C_m$  and the effective length factor  $K$ . Typical columns

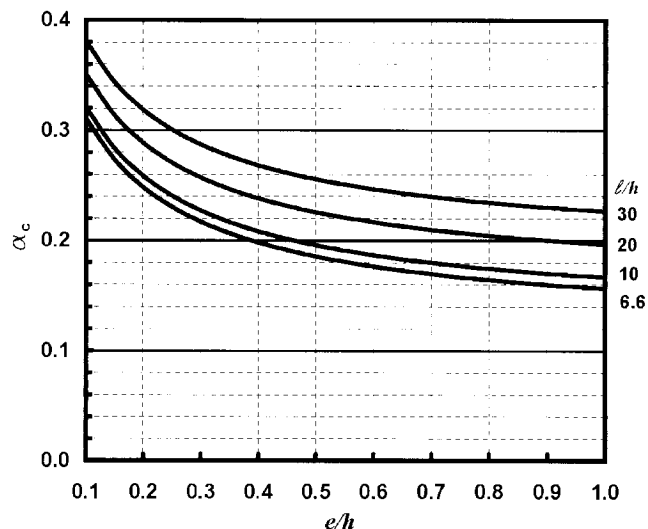


Fig. 13. Graphical solution of  $\alpha_c$  [Eq. (22)] for composite columns

in braced frames would have  $C_m$  factors between 0.6 and 1.0 and  $K$  factors ranging from approximately 0.8 to almost 1.0. The columns in this study were pin-ended and subjected to equal and opposite end moments causing symmetrical single curvature bending, with  $C_m=K=1.0$  (Fig. 1), and represent the most critical condition for columns in braced frames. It is suggested that, for the design of composite columns subjected to major axis bending, the existing ACI design equations for  $EI$  [Eqs. (9) and (10)] be replaced by Eq. (24). It is also suggested that a design aid, similar to Fig. 13, for graphical evaluation of  $\alpha_c$  be placed in the commentary of ACI 318-02 to speed up the design process. Note that the proposed  $EI$  equation was developed from member strengths at ultimate loads and is suitable for that purpose. It should not be used in its current form for pushover analyses or for serviceability calculations, as the equation has not been tested in these areas.

At a glance the proposed  $EI$  equation may look cumbersome. Additionally, it could be argued that the determination of  $e/h$  values from a conventional (first-order) structural analysis may not be accurate enough to justify the additional complexity of Eq. (24). However, if Fig. 13 is employed, the proposed equation is no more complicated than the current ACI  $EI$  equations [Eqs. (9) and (10)]. Furthermore, the use of a spreadsheet will greatly simplify computations regardless of whether the ACI  $EI$  equation or the proposed  $EI$  equation is used.

### Conclusions and Recommendations

This paper presents a statistical evaluation of the parameters that affect the flexural stiffness  $EI$  of slender tied composite steel-concrete columns in which steel shapes are encased in concrete. The columns were subjected to short-term loads and equal end moments causing symmetrical single-curvature bending about the major axis of the encased steel section. The existing ACI 318-02 equations were examined and a new nonlinear equation for  $EI$  [Eq. (24)] was developed from the simulated data. A stiffness reduction factor  $\phi_K=0.85$  is proposed for the new equation. A graphical design aid to speed up computations is also included in this paper.

The results presented in this paper show that the overall variability of the proposed design equation is far lower than that obtained using the current ACI expressions. In addition, the pro-

posed  $EI$  equation is not subject to significant variations due to effects of variables investigated. Note that the proposed  $EI$  equation was developed from member strengths at ultimate loads and is suitable for that purpose.

## Notation

The following symbols are used in this paper:

- $A_g, A_{rs}, A_{ss}$  = area of gross concrete cross-section, of longitudinal reinforcing steel bars, and of structural steel section;
- $C_m$  = equivalent uniform bending moment diagram factor;
- $E_c, E_s$  = moduli of elasticity of concrete and steel;
- $EI$  = effective flexural stiffness of column;
- $EI_{des}$  = flexural stiffness of column computed from design Eqs. (11), (12), and (23);
- $EI_{th}$  = theoretical flexural stiffness of column computed from Eq. (8);
- $e$  = end eccentricity =  $M_2/P_u = M_{col}/P_u$ ;
- $f'_c$  = specified compressive strength of concrete;
- $f_{yrs}, f_{yss}$  = specified yield strength of reinforcing steel bars and of structural steel section;
- $h$  = overall thickness of cross section perpendicular to the axis of bending;
- $I_g, I_{rs}, I_{ss}$  = moment of inertia of gross concrete cross section, of longitudinal reinforcing steel bars, and of structural steel section taken about centroidal axis of composite cross section;
- $K$  = effective length factor;
- $k$  = lowest eigenvalue solution to basic differential equation of equilibrium;
- $\ell$  = unsupported height (length) of member (column);
- $M$  = bending moment;
- $M_c$  = design bending moment, which includes second-order effects;
- $M_{col}, M_{cs}$  = bending moment resistance of member (column) and of cross section;
- $M_{max}$  = maximum bending moment acting along the column length;
- $M_1, M_2$  = smaller and larger of factored moments applied at column ends;
- $n$  = number of data points;
- $P$  = axial load;
- $P_c$  = critical load of column, Eq. (6);
- $P_{cr}$  = Euler's buckling strength or critical load of a pin-ended column, Eq. (4);
- $P_{des}$  = column axial load strength computed from moment magnifier approach;
- $P_o$  = unfactored pure axial load strength of composite cross section;
- $P_{theor}$  = theoretically computed axial load strength of column;
- $P_u$  = factored axial load acting on column;
- $R_c, S_e$  = multiple correlation coefficient and standard error;
- $x_1, x_2$  = independent variables used for regression analyses;
- $\alpha_c, \alpha_{rs}, \alpha_{ss}$  = dimensionless stiffness reduction factors for concrete, for longitudinal reinforcing steel, and for structural steel, respectively;

- $\alpha_k$  = a dimensionless constant;
- $\alpha_1, \alpha_2$  = dimensionless factors corresponding to independent variables  $x_1, x_2$  (or  $e/h, \ell/h$ );
- $\beta_d$  = ratio of the maximum factored axial dead load to the total factored axial load;
- $\Delta_m$  = deflection of column at midheight;
- $\delta_{ns}$  = moment magnifier for columns that are part of braced (nonsway) frames;
- $\delta_1$  = moment magnifier for columns subjected to axial load and equal and opposite end moments causing symmetrical single curvature bending;
- $\rho_{rs}, \rho_{ss}$  = total area of longitudinal reinforcing bars and structural steel section divided by the gross area of concrete cross section;
- $\phi$  = curvature or resistance reduction factor; and
- $\phi_K$  = stiffness reduction factor.

## References

- American Concrete Institute (ACI). (2002). "Building code requirements for structural concrete and commentary." *ACI 318-02 and ACI 318R-02*, Detroit.
- Chen, W. F., and Lui, E. M. (1987). *Structural stability—Theory and implementation*, Elsevier, New York.
- Galambos, T. V. (1963). "Inelastic lateral buckling of beams." *J. Struct. Div. ASCE*, 89(5), 217–242.
- Johnson, R. P., and May, I. M. (1978). "Tests on restrained composite columns." *The Structural Engineer*, Inst. of Engrs., 56B(2), 21–28.
- MacGregor, J. G. (1976). "Safety and limit states design for reinforced concrete." *Can. J. Civ. Eng.*, 3(4), 484–513.
- MacGregor, J. G., Breen, J. B., and Pfrang, E. O. (1970). "Design of slender concrete columns." *ACI Journal, Proceedings*, 67(1), 6–28.
- Mirza, S. A. (1989). "Parametric study of composite column strength variability." *J. Constr. Steel Res.*, 14(2), 121–137.
- Mirza, S. A. (1990). "Flexural stiffness of rectangular reinforced concrete columns." *ACI Struct. J.*, 87(4), 425–435.
- Mirza, S. A., Lee, P. M., and Morgan, D. L. (1987). "ACI stability resistance factor for RC columns." *J. Struct. Eng.*, 113(9), 1963–1976.
- Mirza, S. A., and MacGregor, J. G. (1982). "Probabilistic study of strength of reinforced concrete members." *Can. J. Civ. Eng.*, 9(3), 431–448.
- Mirza, S. A., and Skrabek, B. W. (1991). "Reliability of short composite beam-column strength interaction." *J. Struct. Eng.*, 117(8), 2320–2339.
- Mirza, S. A., and Skrabek, B. W. (1992). "Statistical analysis of slender composite beam-column strength." *J. Struct. Eng.*, 118(5), 1312–1332.
- Mirza, S. A., and Tikka, T. K. (1999a). "Flexural stiffness of composite columns subjected to major axis bending." *ACI Struct. J.*, 96(1), 19–28.
- Mirza, S. A., and Tikka, T. K. (1999b). "Flexural stiffness of composite columns subjected to bending about the minor axis of structural steel section core." *ACI Struct. J.*, 96(5), 748–756.
- Morino, S., Matsui, C., and Watanabe, H. (1984). "Strength of biaxially loaded SRC columns." *Composite and Mixed Construction*, 241–253.
- Newmark, N. M. (1943). "Numerical procedure for computing deflections, moments, and buckling loads." *ASCE Transactions*, 108, 1161–1234.
- Park, R., Priestly, M. J. N., and Gill, W. D. (1982). "Ductility of square-confined concrete columns." *J. Struct. Div. ASCE*, 108(4), 929–950.
- Procter, A. N. (1967). "Full size tests facilitate derivation of reliable design methods." *The Consulting Engineer*, 31(8), 54–60.
- Roik, K., and Mangerig, I. (1987). "Experimentelle Untersuchungen der Tragfähigkeit von einbetonierten Stahlprofilstützen unter besonderer

- Berücksichtigung des Langzeitverhaltens von Beton." Bericht zu P102, Studiengesellschaft für Anwendungstechnik von Eisen und Stahl e.V., Düsseldorf, Germany, 83 pp.
- Roik, K. H., and Schwalbenhofer, K. (1988). "Experimentelle Untersuchungen zum plastischen Verhalten von Verbundstützen." Bericht zu P125, Studiengesellschaft für Anwendungstechnik von Eisen und Stahl e.V., Düsseldorf, Germany, 196 pp.
- Suzuki, T., Takiguchi, K., Ichinose, T., and Okamoto, T. (1984). "Effects of hoop reinforcement in steel and reinforced concrete composite sections." *Bulletin of the New Zealand National Society for Earthquake Engineering*, 17(3), 198–214.
- Tikka, T. K., and Mirza, S. A. (2004). "Equivalent uniform moment diagram factor for reinforced concrete columns." *ACI Struct. J.*, 101(4), 521–531.
- Timoshenko, S. P., and Gere, J. M. (1961). *Theory of elastic stability*, 2nd Ed., McGraw-Hill, New York.
- Young, B. W. (1971). "Residual stresses in hot rolled sections." *Report No. CUED/C-Struct/TR.8*, Dept. of Engineering, Univ. of Cambridge, London.